*Progress In Electromagnetics Research C, Vol. 112, 239–250, 2021*

# A Comparative Study of Some Novel Wideband Tulip Flower Monopole Antennas with Modified Patch and Ground Plane

**Nurhayati Nurhayati[1, *], Alexandre M. De-Oliveira[2], Warangkana Chaihongsa[3], Bagus E. Sukoco[4], and Akbar K. Saleh[5]**

**Abstract**—Comparative study of some novel wideband Tulip Flower Monopole Antennas (TFMAs) is presented in this paper. To Improve the bandwidth and increase the gain, modification of the shape of the curves and slots in the patch and ground plane was carried out on the seven TFMAs. TFMA-A, TFMA-B, TFMA-C, and TFMA-D have dimensions of $50 \times 50\,\text{mm}^2$, while TFMA-E, TFMA-F, and TFMA-G have dimensions of $30 \times 70\,\text{mm}^2$. From the simulation result, TFMA-A operated from 2 GHz to more than 30 GHz with a return loss of 15 dB occupies most of its operating frequency. In the whole frequency work, the peak directivity performance in the order of superiority is obtained for TFMA-G, TFMA-F, TFMA-D, TFMA-E, TFMA-C, TFMA-B, and TFMA-A. The improvement of directivity is reached for TFMA-D of 5.03 if it is compared to TFMA-A at 24 GHz. TFMA-G obtains the peak of directivity of 10.148 dBi at 23 GHz. The impedance bandwidth and directivity of the antenna element change by varying the curvature, the shape, and the position of slot in the radiator and ground plane also the height of the microstrip feeding line and ground plane. The return losses of the TFMA-A and TFMA-E show good agreement between simulation and measurement results.

## 1. INTRODUCTION

In recent years, the need for telecommunication have always been developed rapidly. All telecommunication devices such as smartphones, tablets, laptops, and Internet of Things (IoT) devices require high-speed data transmission to upload and download data. Antenna as the front end of the telecommunication system plays an important role for sending or receiving data. Due to the increasing need for data transfer capacity, telecommunication equipment requires a large bandwidth for this purpose. Apart from telecommunications, radar applications also require a wide band antenna as an object detection sensor. The research discussing wide-band and multi-band antennas that support high rate data transmission has also grown. The antenna designed for Wireless Local Area Network (WLAN) operating in 2.4 GHz, 5.2/5.8 GHz, Worldwide interoperability for Microwave Access (WiMax) operating at 2.5/3.5/5.5 GHz (Long Term Evolution) LTE and (Global System for Mobile Communication) GSM application has been reported in [1–3].

Monopole antennas that support IEEE 802.11a/b/g with disk-slit shaped [4], ring fractal [5] U and L-slot [6], rectangular, T-shaped [7], log-periodic [8], vertical stub, and horizontal slit [9] have been discussed for mobile communication. All of the antennas only cover several multi-band frequencies in the S or C band application with sufficient impedance bandwidth. The application of telecommunication at high-frequency band, i.e., Ku band (12.4–18 GHz) and K-band (18–26.5 GHz) by square patch antenna

*Received 7 April 2021, Accepted 14 May 2021, Scheduled 18 May 2021*
* Corresponding author: Nurhayati Nurhayati (nurhayati@unesa.ac.id).
[1] Department of Electrical Engineering, Faculty of Engineering, Universitas Negeri Surabaya, Indonesia, Surabaya 60231, Indonesia. [2] Maxwell Laboratory of Microwave and Applied Electromagnetism of the Federal Institute of São Paulo, IFSP, Suzano — SP, Brazil. [3] DKK Denki Kogya Co, Ltd, Kanuma, Japan. [4] Lembaga Ilmu Pengetahuan Indonesia (LIPI), Electronics and Telecommunications Center, Bandung, Indonesia. [5] Department of Electrical Engineering, Faculty of Engineering, Universitas Negeri Surabaya, Indonesia, Surabaya 60231, Indonesia.

which provides diversity has been reported in [10]. Low profile antennas with Bull's Eye [11], conical monopole [12], array antenna [13], half Yagi [14], microstrip band notch [15] have also been discussed for microwave communication such as radar and satellite communication in Ka and Ku band applications. The requirement of frequency radio that covers multiband or wide-band frequency is also needed for Radio Armature, Global Positioning System (GPS), GSM, Personal Service Communication (PCS), Industry Scientific and Medical (ISM), blue-tooth, astronomy, automotive radar, radio navigation [16–19] and others. Moreover, the ultra-wide-band technology that works in the 3.1 to 10.6 GHz [20] frequency has been widely used in Wireless Personal Area Networks (WPAN). Some of the antennas operating at the UWB frequency have the low end frequency around 3 GHz and high end frequency around 10 GHz, with some large antenna sizes, not cover all of UWB frequency with the high impedance bandwidth, and have a small peak gain.

The high need for data communication encourages researchers to examine devices that can cover frequency Super Wide Band (SWB) technology. It can also cover short-range communications including various telecommunication application services and radar technology which has a bandwidth impedance of at least 10 : 1. The previous research about SWB has been done by fractal antenna [21] and band-notch monopole antenna [22]. It has a notched band in frequency 4.7–6 GHz. SWB antenna has also been designed with semi elliptically fractal and gets the impedance bandwidth 172% with dimension $35 \times 77\,\text{mm}^2$ [23]. A CPW-fed antenna with circular triangular patch shape has been discussed in [24] that can be operated in 4.9–25 GHz. SWB monopole antennas have also been discussed in [25, 26]. All of the monopole antennas have different characteristics with specific complicated designs and frequencies.

In this article, we design seven novel low-profile Wideband Tulip Flower Monopole antennas (TFMAs) that has high impedance bandwidth and high performance of gain. The comparative study of seven novel TFMAs by modifying the curvature and optimizing patch and ground plane has been done to get return loss, surface current, and radiation pattern performance. TFMA-A has the superiority in impedance bandwidth that covers frequency 2 GHz to more than 30 GHz. It has $S_{11}$ less than $-15$ dB for most of the frequency band. An increase in the directivity occurs with 5.03 dBi for TFMA-D compared to TFMA-A at 24 GHz. By modifying patch and ground plane, there is increase in gain, especially in the high-frequency band. Our antenna has novelty in shape, high impedance bandwidth (TFMA-A), and high peak gain (TFMA-G) with low profile size.

This paper is organized into six sections. The design, shape, and dimension of seven novel antennas are presented in Section 2. The return loss, surface current, and radiation pattern performance ofb the antennas are explored in Section 3. The measurement result and comparative result are delivered in Sections 4 and 5. The last section is conclusion.

## 2. ANTENNA DESIGN

Seven models of TFMA are shown in Figure 1, and the dimension is denoted in Table 1. The antennas are designed by FR4 substrates, with a dimension of $50 \times 50\,\text{mm}^2$ for TFMA A-D and $30 \times 70\,\text{mm}^2$ for

**Table 1.** Parameter dimension of the antenna.

| Parameter dimension in mm | | | | | | | |
|---|---|---|---|---|---|---|---|
| Par | Dim | Par | Dim | Par | Dim | Par | Dim |
| $a$ | 50 | $i$ | 18.6 | $q$ | 10 | $C$ | 17 |
| $b$ | 50 | $j$ | 27.5 | $r$ | 29.6 | $D$ | 12 |
| $c$ | 19.5 | $k$ | 10 | $s$ | 15.5 | $E$ | 17.5 |
| $d$ | 17 | $l$ | 7.15 | $t$ | 12.6 | $F$ | 29.5 |
| $e$ | 3 | $m$ | 13 | $u$ | 3 | $G$ | 5 |
| $f$ | 2 | $n$ | 18 | $v$ | 14 | $H$ | 5 |
| $g$ | 27.5 | $o$ | 7 | $A$ | 70 | $I$ | 0.5 |
| $h$ | 10 | $p$ | 27.5 | $B$ | 30 | $J$ | 25 |

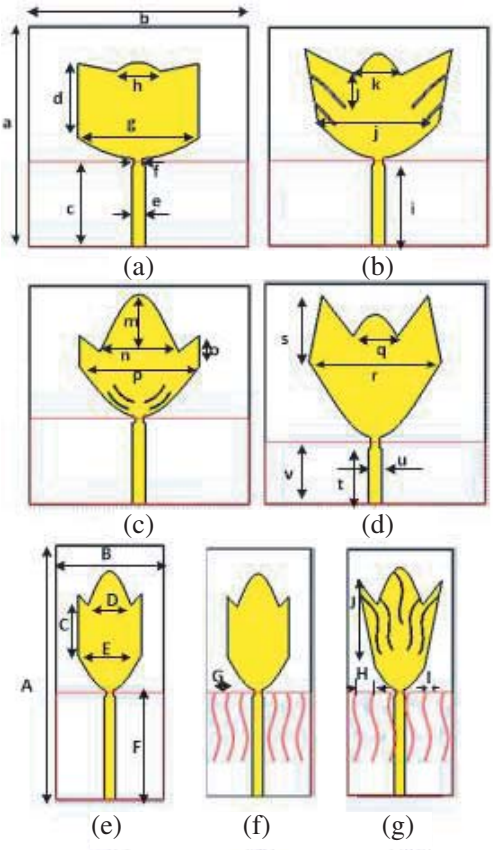


**Figure 1.** Geometry of seven Tulip Flower Monopole Antenna (TFMA), (a) TFMA-A, (b) TFMA-B, (c) TFMA-C, (d) TFMA-D, (e) TFMA-E, (f) TFMA-F and (g) TFMA-G.

TFMA E-G. All of the antennas have different shapes of patch or ground plane designed by CST Studio Suite.

To get higher impedance bandwidth in the lower frequency and enhance the gain, we modify the patch and ground of the antenna. The feeding transmission line has a bottle neck that has a width of 2 mm while the feed has a width dimension of 3 mm. We also add a gap between the radiator and the ground. There are different shapes of curvature in the patch and ground plane which follow the function.

$$f(t) = K_1\left(K_2 + K_3\cos\left(\frac{K_4\pi t}{K_5}\right)\right) \tag{1}$$

The tapered curve and slot in the patch and ground plane of the antenna use Equation (2). On the lower side of the TFMA-A, the bottom radiator curve has $K_1 = 25$, $K_2 = 0.5$, $K_3 = 0.5$, $K_4 = 0.75$, and $K_5 = 36$. The lower side of the curved shapes for TFMA has the value of $t$ varied from $-13.75$ to 13.75. But for the upper side radiator curve has $K_1 = 20$, $K_2 = 0.5$, $K_3 = -0.5$, $K_4 = 1.25$, and $K_5 = 36$ with $t$ varied from $-5$ to 5. The tapered curve is greatly influenced by all of the constants. The higher the value of $K_4$ is, the deeper the curvature is, but it also depends on the value of the range of $t$.

The percentage bandwidth can be found by [27], and Bandwidth Dimension Ratio (BDR) can be expressed in Equation (1) by [23].

$$BDR = \frac{BW\%}{\lambda_{Length} \times \lambda_{Width}} = \frac{\left({}^{2(f_h - f_l)}/_{f_u + f_l}\right) \times 100\%}{\left({}^{L}/_{(c/f_l)}\right) \times \left(\left({}^{W}/_{(c/f_l)}\right)\right)} \tag{2}$$

$BW$ is the percentage of bandwidth, $f_l$ the lowest frequency, $f_h$ the highest frequency, $L$ the length of the antenna, $W$ the width of the antenna, $c$ the light speed in the vacuum, and $\lambda$ the wavelength relative to the lowest frequency work.

## 3. RESULT AND DISCUSSION

### 3.1. Return Loss Performance

The return loss performance of the seven novel antennas can be seen in Figures 2(a)–(d) and Figures 3(a)–(c). All of the antennas have been designed and simulated between the lowest frequency of 1 GHz and the highest frequency of 30 GHz. All of the antennas have different performances of return loss. TFMA A-D have a dimension $50 \times 50\,\text{mm}^2$ as shown in Figure 2, and TFMA E-G have a dimension of $30 \times 70\,\text{mm}^2$. The width of TFMA A-D is larger than TFMA E-G, and it influences the performance of return loss in the low frequency. The wider the width is, the better performance the return loss is in the low frequency and vice versa. With the same width of the substrate, the shape of the radiator and ground plane also influence the return loss performance. TFMA-A has the best impedance bandwidth in the SWB frequency. It has a return loss better than 15 dB almost in the entire operating frequency (2–30 GHz).

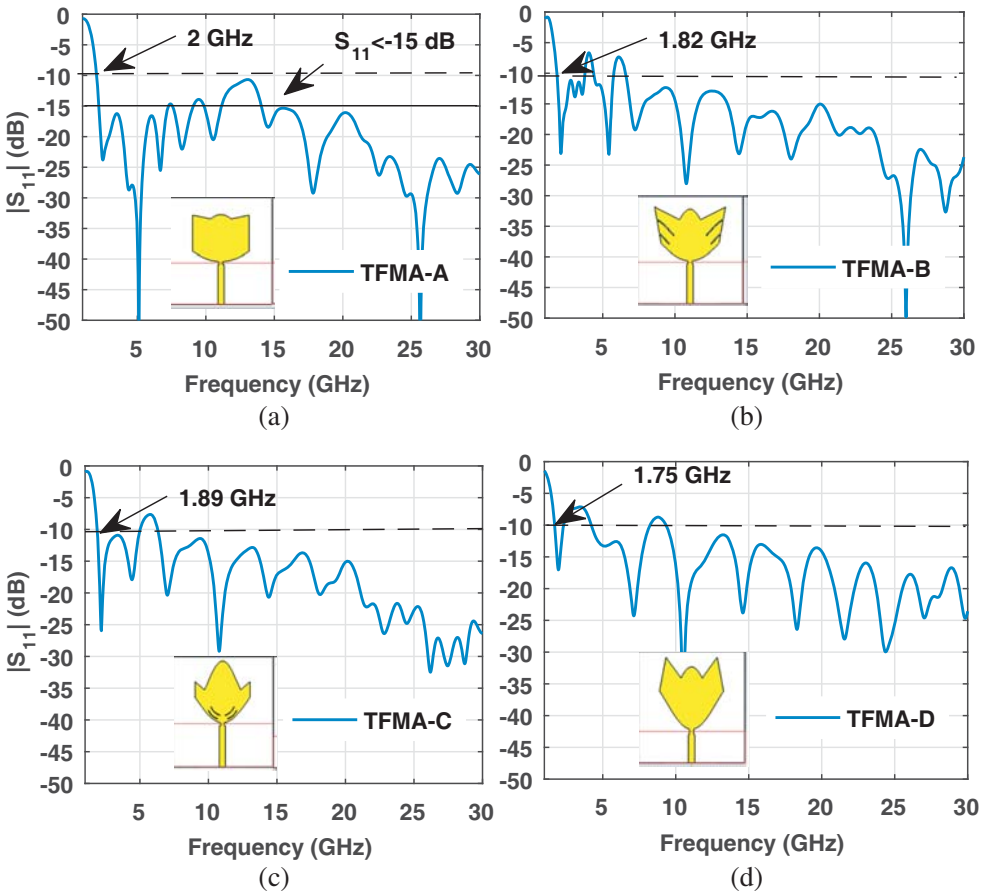


**Figure 2.** Return Loss performance of (a) TFMA-A, (b) TFMA-B, (c) TFMA-C and (d) TFMA-D.

Better return loss in the low-end frequency is obtained for TFMA-D, TFMA-B, TFMA-C, and TFMA-A, respectively. TFMA-D has a lower height of the ground plane than another structure, and it has a narrower and deeper curvature on the bottom side. It influences the return loss in the low-end frequency. Although TFMA-D has a better performance of return loss in low-end frequency, TFMA-A reaches the best performance of impedance bandwidth in the whole of frequency.

The return losses of TFMA F-G are shown in Figures 3(a)–(c). The narrower the width is, the longer the height of the antenna size is, the worse the performance of the return loss is in some frequencies. Although the return loss gets a better performance in the lower frequency, some of the frequency does not cover the impedance bandwidth 10 dB across the operating frequencies. Better return loss for

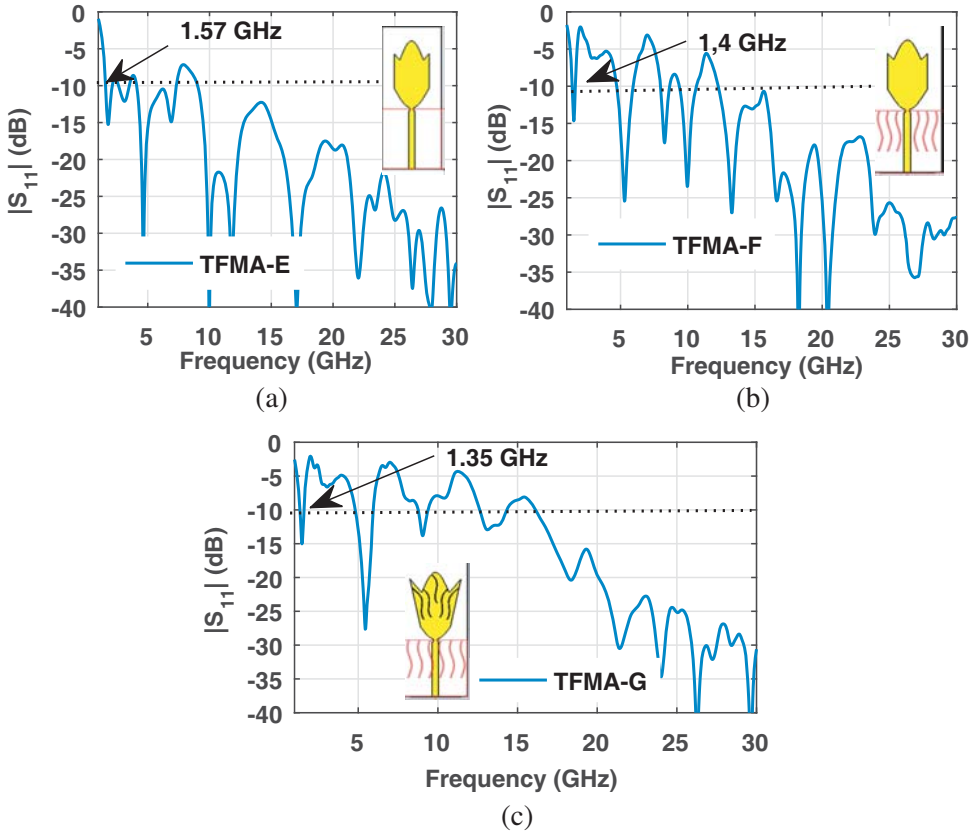


**Figure 3.** Return loss performance of (a) TFMA-E, (b) TFMA-F and (c) TFMA-G.

$30 \times 70\,\text{mm}^2$ in the low-end frequency is reached for TFMA-G, TFMA-F, and TFMA-E, i.e., 1.35 GHz, 1.4 GHz, and 1.57 GHz. The simulation shows that a smaller width of the element yields a better performance of return loss in the high-end frequency. Figures 3(b) and (c) show the different shapes of ground plane structure for TFMA-E and TFMA-F. TFMA-G has different shapes of the radiator and also the ground plane with TFMA-E. We add some slot structures in the ground plane as shown in Figure 3(b) and slot structures in the radiator as displayed in Figure 3(c). The different performances of return loss, surface current, and radiation pattern of the antenna are shown from that structure. The electric field excited in the microstrip line changes by the narrower width of the element and slot structured in the ground plane.

### 3.2. Surface Current Performance

The surface current in the antenna shows the amount of electric charge per unit time in the cross-sectional area. It also describes the orientation direction of current in that area. The more surface current also denotes the stronger electric field distribution in that area.

Figure 4 exposes the surface current distributions for TFMA-A, TFMA-D, TFMA-E, and TFMA-G at 5 GHz. In Figure 4(a), it can be seen that TFMA-A has surface currents that are evenly distributed across all patches and ground. Figure 3(b) shows the surface current strongly focused around the two edge side of the radiator in TFMA-D. TFMA-D has a lower height of the ground and a deeper tapered curve than TFMA-A. It influences the resonance at each frequency and the flowing of surface current. Figures 4(c)–(d) show the differences of surface current for TFMA-E and TFMA-G that have a dimension of $30 \times 70\,\text{mm}^2$. TFMA-G has more surface currents in the curved slot than any other structures in the patch and ground plane. With the wave structure of the slot and also the shape of curvature of the radiator, the surface current will be trapped in the structure, and it will affect the resonance frequency and gain.

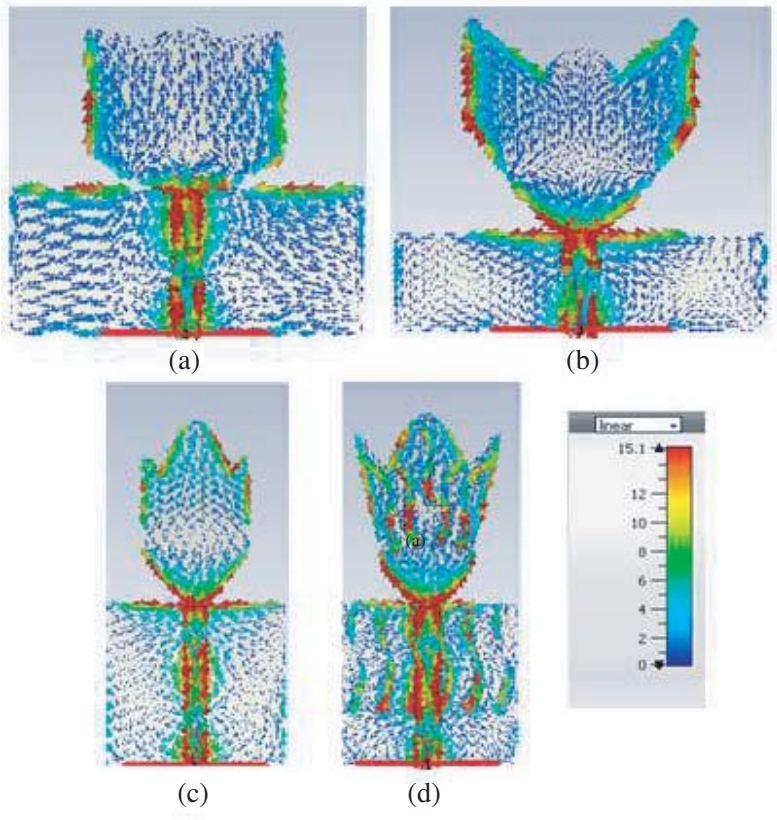


**Figure 4.** Surface current of: (a) TFMA-A, (b) TFMA-D, (c) TFMA-E and (d) TFMA-G.

### 3.3. Radiation Pattern Performance

The radiation patterns of some TFMAs are shown in Figure 5 in the $E$-plane at theta 90°. Figure 5(a) shows the radiation patterns at frequency 5 GHz for TFMA-B and TFMA-C. TFMA-B has a directivity of 3.54 dBi with a side lobe level (SLL) of −4 dB, but TFMA-C has a directivity of 5.58 dBi with SLL −5.7 dBi. It indicates that TFMA-C has higher directivity and better performance of SLL than TFMA-B. TFMA-C has a deeper curvature in the bottom side and upper side of the radiator. Figure 5(b) shows that at 11 GHz, TFMA-A has directivity 3.88 dBi and SLL −0.5 dB with main lobe direction 31 deg. However, TFMA-D has directivity 7.1 dBi and SLL −4.2 with main lobe direction 146 deg. At 24 GHz, TFMA-A has directivity 3.82 dBi, main lobe 104 deg, and SLL −1.3 dB. TFMA-D has directivity 8.65 dBi, SLL −3.4 dB, and main lobe direction 98 deg.

TFMA-D has superiority of directivity and SLL level if it is compared with TFMA-A at 11 GHz and 24 GHz. The deeper the antenna curvature is, the more the surface current is on it, and it yields resonance at 11 GHz and 24 GHz. At 11 GHz, the antenna can be applied to X-band application as radar, satellite communication, and space communication. At frequency 24 GHz, thr antenna can be applied to automotive radar application, ISM band, and Wireless Sensor Network (WSN) application. Figure 5(d) shows that at 8 GHz TFMA-F has directivity 2.67 dBi, SLL −4.4 dB, and main lobe direction −65 deg, and TFMA-E has directivity 5.49 dBi, main lobe direction 120 deg, and SLL −1.4 dB. At 24 GHz, TFMA-F has directivity 5.92 dBi and SLL −2.8 dB while TFMA-G has directivity 9.61 dBi and SLL −2.5 dBi. Different shapes of the ground and patch can influence the resonant frequency, even though TFMA-E, F, and G have the same dimension of the substrate. The slot structure in the ground and patch of the antenna can improve antenna directivity, especially in high frequency.

Figure 6 displays the maximum directivities of TFMA-A to D for frequencies 1–30 GHz. At frequency 5 GHz, TFMA-B has directivity 3.54 GHz, but TFMA-C has directivity 5.58 GHz. At 11 GHz, TFMA-A has directivity 3.88 dBi, and TFMA-D has directivity 7.1 dBi. It has an improvement of

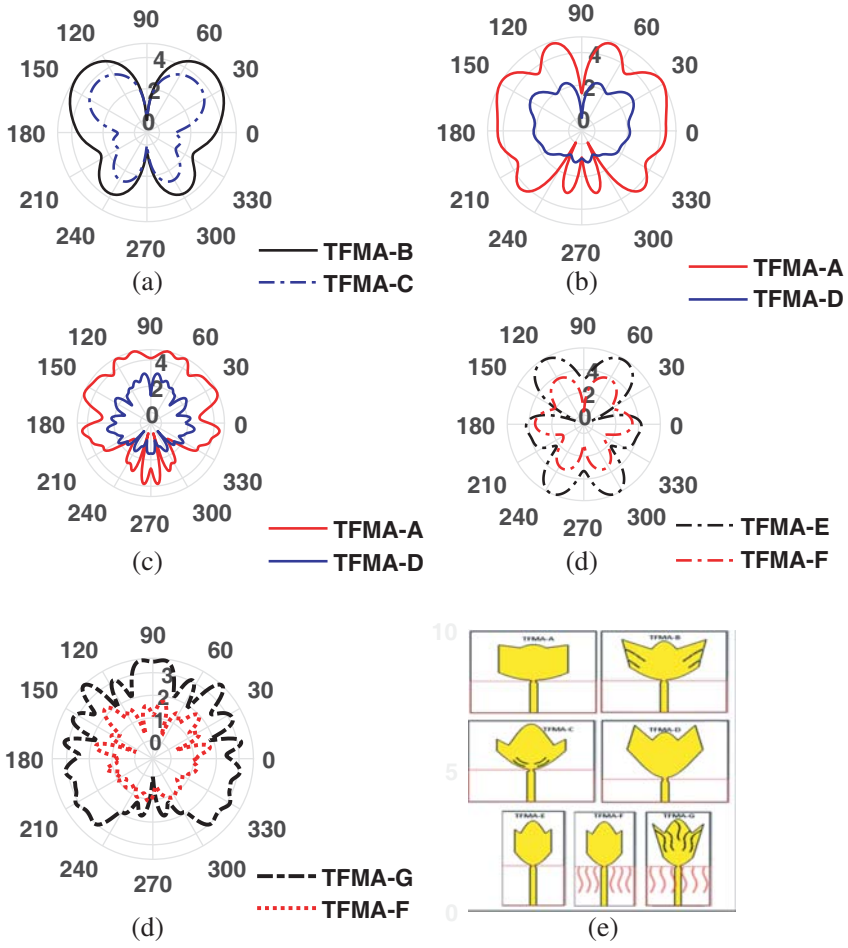


**Figure 5.** Polar plot in the *E*-plane at theta 90° for (a) TFMA-B and TFMA-C at 5 GHz, (b) TFMA-A and TFMA-D at 11 GHz, (c) TFMA-A and TFMA-D at 24 GHz, (d) TFMA-F and TFMA-E at 8 GHz, (e) TFMA-F and TFMA-G at 24 GHz and (d) antenna types.

directivity of 3.22 dBi. The improvement of directivity of 5.03 dBi is obtained for TFMA-D if it is compared to TFMA-A at 24 GHz. The highest directivity reaches 9.45 dBi for TFMA-D, while TFMA-A has a directivity 3.86 dBi at 27 GHz. It has the improvement of directivity of 5.59 dBi. In almost all parts of the frequency from 10 GHz to 30 GHz, the sequence of directivity from worst to better is reached for TFMA-A, TFMA-B, TFMA-C, and TFMA-D.

Figure 7 shows the directivities for TFMA-E to TFMA-G. At 8 GHz, TFMA-F has directivity 2.67, and TFMA-E has directivity 5.49 dBi. It has an improvement of directivity of 2.82 dBi. For 24 GHz, TFMA-F has a directivity of 5.92 while TFMA-G has a directivity of 9.61 GHz. It means that there is increase in the directivity of 3.69 dBi. The highest directivity for an antenna with the size $30 \times 70\,\text{mm}^2$ is reached for TFMA-G as 10.148 dBi for 23 GHz. Reducing the width of the antenna will affect the resonance of the lower frequencies, but it improves the impedance bandwidth performance at the upper frequencies. Changing the curvature of the TFMA curve and providing a slot structure can improve antenna directivity, especially at high frequencies. However, dedicating a slot structure will also affect the impedance at low frequencies.

Figure 6 and Figure 7 show that the variation of directivity in frequency 1–30 GHz is relatively high. It could be generated by the tapered curve, the existence of sharp construction, and the slot shape of the radiator patch and ground plane that influence the electric field in each frequency. Minimizing the variation of gain could be achieved by changing the variation of the tapered curve and slot of the radiator and ground plane. However, there is an improvement of directivity of 5.59 dBi for TFMA-D compared to

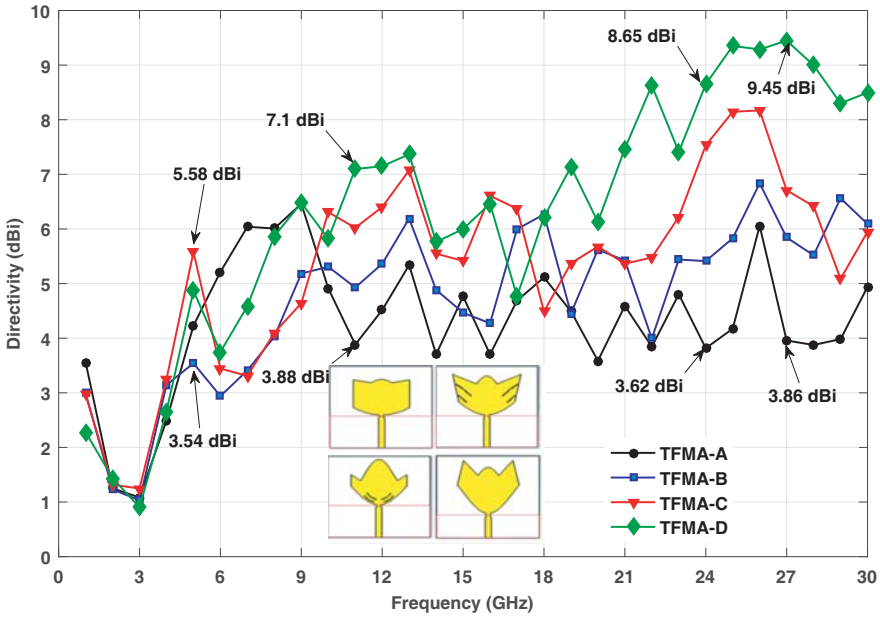


**Figure 6.** Directivity of TFMA-A, TFMA-B, TFMA-C and TFMA-D in the *E*-plane at Theta 90°.

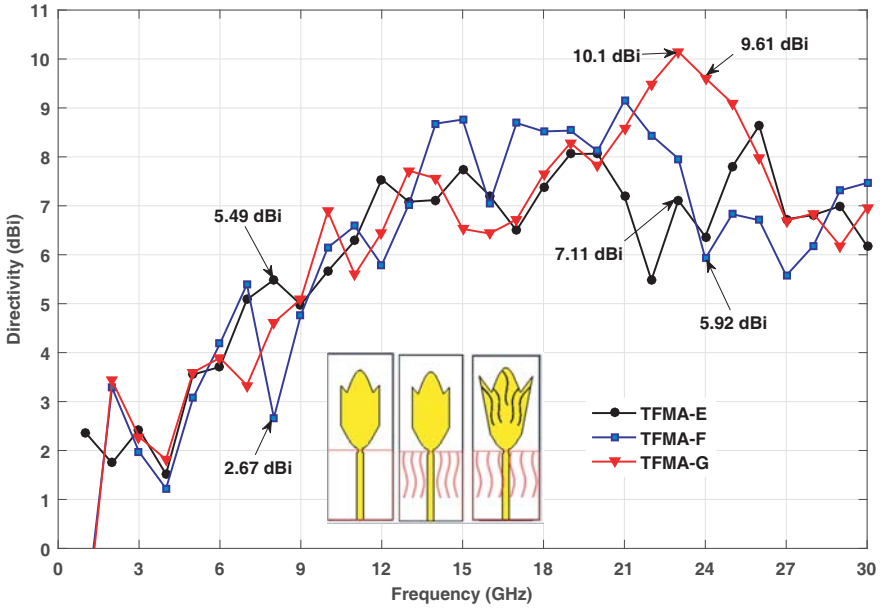


**Figure 7.** Directivity of TFMA-E, TFMA-F and TFMA-G in the *E*-plane at Theta 90°.

TFMA-A at 27 GHz. Although the TFMA has various performances of directivity in different frequencies for different models, it could be considered for being applied to wireless communication, 5G, and radar application. It can also be developed for the next research to get a better performance of return loss and stable radiation pattern performance in the Super Wide Band frequency.

## 4. MEASUREMENT RESULT

Figure 8 shows the antenna fabrication result for TFMA-A and TFMA-E. We only fabricated TFMA-A and TFMA-E because TFMA-A and TFMA-E have the best impedance bandwidth in most frequency.

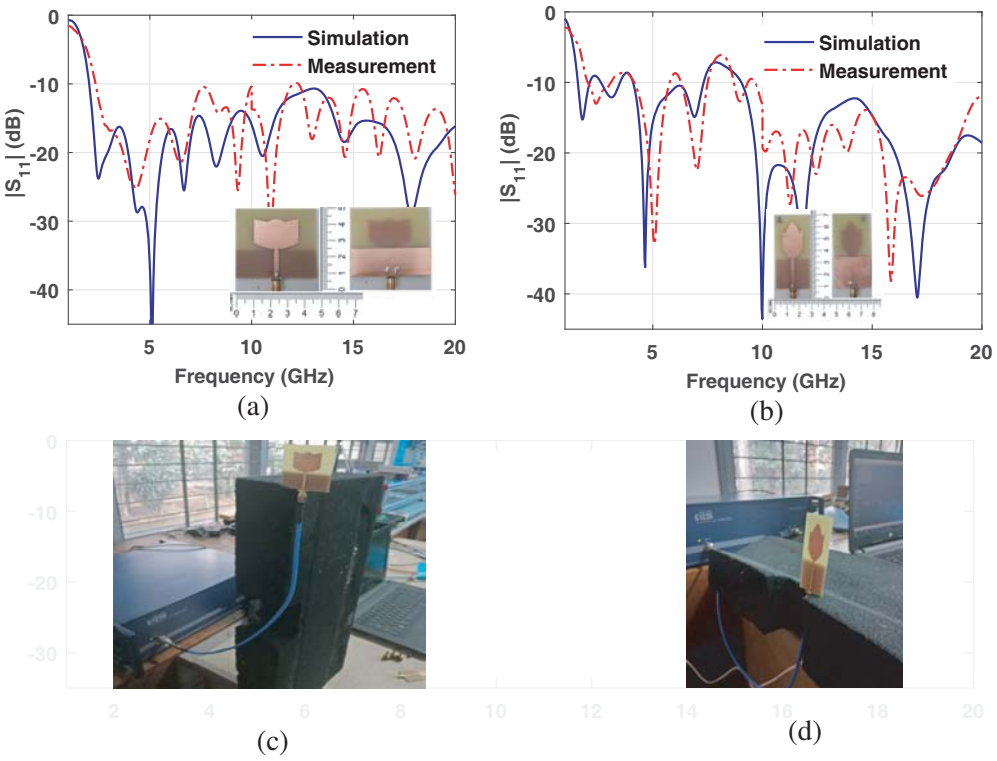


**Figure 8.** Measurement result of (a) TFMA-A, (b) TFMA-E, (c) TFMA-A and (d) TFMA-E.

Although another shape has better directivity in high frequency, the return loss better than 10 dB is only achieved for TFMA-A and TFMA-E. We measure the $S_{11}$ of the two antennas by Vector Network Analyzer (VNA) Copper Mountain C1220 (Cobalt type) that has a frequency range of 100 kHz to 20 GHz. From the measurement, there is an agreement between simulation and measurement, especially in the low frequency. In high frequency, there are some different results for simulation and measurement. The discrepancy between the simulation and measurement results can be caused by the limited VNA frequency range, substrate types, the quality of the SMA connector, the cable type, the range of frequency work, and the calibration of the VNA. The interference and the distinction in resonance between the simulation and measurement results is due to the measurement not being carried out in an anechoic chamber. We use FR4 material which is very easy to obtain and cheap, but it is less suitable for high-frequency applications. This article only reports the results that have been obtained and can be used to develop future research.

## 5. COMPARATIVE RESULT

Table 2 shows the comparison performance results of TFMA-A, TFMA-B, TFMA-C, TFMA-D, TFMA-E, TFMA-F, and TFMA-G and some previous literature studies that use the same substrate type. From Table 2, we can see that references [1–5] have a smaller area of the substrate than our purposes. Even though they have a smaller area, they cannot cover all bandwidths to get the return loss of 10 dB and can just work until 12 GHz. Reference [1] has the peak gain just reaching 3.74 dBi. Reference [21] can be operated up to 26 GHz, and it has a lower-end frequency range, but it has a larger area of the substrate than our purpose. Reference [23] has better BDR than others, but it can just operate until 12 GHz, and it has a larger dimension area than our purpose. We do not report the BDR in the table for all the comparative antennas because some of the antennas do not cover all frequency bands. TFMA-A has BDR 1924; however, reference [23] has BDR 2613. Although [23] has better BDR than TFMA-A, [23] has a larger area and covers only up to 12 GHz. TFMA-A can cover more than 30 GHz with good impedance bandwidth in high-end frequency. It also has a return loss of 15 dB in most of the operating

**Table 2.** Comparison of modelling and simulation result.

| Ref./ Ant. | Size in $mm^2$ | Subs/thick in mm | BW in GHz | Peak Gain |
|---|---|---|---|---|
| [1] | $29 \times 21$ (609) | FR4/1.6 | 2.39–2.51<br>3.38–3.72<br>4.79–6.24 | 3.74 dBi |
| [2] | $25 \times 25$ (625) | FR4/0.8 | 2.4–12.9 | 3.4 dB |
| [4] | $24 \times 31$ (751) | FR4/1.6 | 2.4–2.484<br>5.12–5.825 | 1.18 dBi (2.4 GHz) |
| [5] | $25 \times 25$ (625) | FR4/1 | 2.42–3<br>3.3–4.25<br>5.1–7.2 | 1.08 dBi (5.8 GHz) |
| [21] | $62 \times 64$ (3968) | FR4/1.58 | 1.68–26 | 5.5 dBi (24 GHz) |
| [23] | $77 \times 35$ (2695) | FR4/1.6 | 1.44–12 | 7 dBi |
| [26] | $30 \times 40$ (1200) | FR4/1.6 | 2.5–80 | 5.9 dBi |
| TFMA-A | $50 \times 50$ (2500) | FR4/1.6 | 2–30 | 6.46 dBi (9 GHz) |
| TFMA-B | $50 \times 50$ (2500) | FR4/1.6 | 1.82–3.76<br>4.37–5.75<br>6.58–30 | 6.83 dBi (26 GHz) |
| TFMA-C | $50 \times 50$ (2500) | FR4/1.6 | 1.89–5<br>6.29–30 | 8.15 dBi (25 GHz) |
| TFMA-D | $50 \times 50$ (2500) | FR4/1.6 | 1.75–2.31<br>4.22–8.22<br>9.34–30 | 9.35 (25 GHz) |
| TFMA-E | $70 \times 30$ (2100) | FR4/1.6 | 1.57–3.5<br>4.1–7.31<br>9.04–30 | 8.63 dBi (26 GHz) |
| TFMA-F | $70 \times 30$ (2100) | FR4/1.6 | 1.4–1.63<br>4.7–5.92<br>7.97–10.63<br>12.27–30 | 9.14 dBi (21 GHz) |
| TFMA-G | $70 \times 30$ (2100) | FR4/1.6 | 1.35–1.58<br>4.8–5.9<br>8.7–9.9<br>12.63–30 | 10.148 dBi (23 GHz) |

frequencies from 2 to more than 30 GHz. If TFMA-E can cover the entire frequency range from 2 to 10 GHz it will have BDR 3131.57. It is indicated that it has a higher BDR than [23]. But our TFMA-E, F, G do not cover all of the frequency bands especially in the low-frequency range, so for the next work it needs to optimize the parameter by varying parameter $K_n$ (see Equation (2)) or the slot position. Reference [26] has the largest frequency range, and it has a smaller area than our purpose, but it just earns the maximum gain of 5.9 dBi. Our purpose can reach the peak directivity/gain up to 10.148 dBi

(at 23 GHz). The area of the substrate influences the peak gain. Although the antenna has the same area, they show different impedance bandwidths and peak gains. The presence of slot in the ground plane and radiator will affect the TFMA performance. Moreover, the size of the substrate, the height of the ground plane, the shape of the patch curvature, and the feeding shape also influence the bandwidth and the directivity performance of the antenna.

## 6. CONCLUSION

A comparative study of seven Novel Tulip Flower Monopole Antennas (TFMAs) has been done to know the bandwidth and radiation pattern performance. The modification and optimization of the curvature, the shape of the slot structure, and the height of feeding shape and ground plane affect the bandwidth impedance and peak gain. The best impedance bandwidth is achieved for TFMA-A from 2 to 0 GHz with $S_{11} < -15$ dB at most operating frequencies. The peak gain is reached for TFMA-G of 10.148 dBi at 23 GHz. TFMA can be used in a UWB or SWB application in single element or array antenna which is versatile for the development of telecommunication or radar applications.

## ACKNOWLEDGMENT

We would like to appreciate this work to the Ministry of Research and Technology/National Research and Innovation (Kemenristek-BRIN) of the Republic of Indonesia and LPPM Universitas Negeri Surabaya through Directorate Research and Community Service contract No.288/SP2H/LT/DRPM/202 and LoA of Rectore of Universitas Negeri Surabaya, No.409/UN38/HK /PP/2O21. This Research is a collaboration between Antenna and propagation Laboratory, Departement of Electrical Engineering, Faculty of Engineering, Universitas Negeri Surabaya, Indonesia and Maxwell Laboratory IFSP, Brazil, LIPI and ITB Bandung, Indonesia.

## REFERENCES

1. Chen, H., X. Yang, Y. Z. Yin, S. T. Fan, and J. J. Wu, "Triband planar monopole antenna with compact radiator for WLAN/WiMAX applications," *IEEE Antennas and Wireless Propagation Letters*, Vol. 12, 1440–1443, 2013.
2. Zehforoosh, Y. and T. Sedghi, "An improved CPW-fed printed UWB antenna with controllable band-notched functions," *Journal of Communication Engineering*, Vol. 5, No. 1, 38–49, 2016.
3. Liu, Y., P. Liu, Z. Meng, L. Wang, and Y. Li,, "A planar printed nona-band loop-monopole reconfigurable antenna for mobile handsets," *IEEE Antennas and Wireless Propagation Letters*, Vol. 17, No. 8, 1575–1579, 2018.
4. Liu, C. S., C. N. Chiu, and S. M. Deng, "A compact disc-slit monopole antenna for mobile devices," *IEEE Antennas and Wireless Propagation Letters*, Vol. 7, 251–254, 2008.
5. Pourahmadazar, J., C. Ghobadi, J. Nourinia, and H. Shirzad, "Multiband ring fractal monopole antenna for mobile devices," *IEEE Antennas and Wireless Propagation Letters*, Vol. 9, No. 1, 863–866, 2010.
6. Moosazadeh, M. and S. Kharkovsky, "Compact and small planar monopole antenna with symmetrical L- and U-shaped slots for WLAN/WiMAX applications," *IEEE Antennas and Wireless Propagation Letters*, Vol. 13, 388–391, 2014.
7. Zhu, Y., F. S. Zhang, C. Lin, Y. C. Jiao, and R. Zou, "Design of a compact dual-band printed monopole antenna for WLAN applications," *2010 9th Int. Symp. Antennas Propag. EM Theory, ISAPE 2010*, 1–3, 2010.
8. Li, J., Y. Huang, G. Wen, L. Ma, W. Hu, and W. Gu, "A six-octave wideband and low profile log-period monopole endfire antenna," *2018 IEEE Antennas Propag. Soc. Int. Symp. Usn. Natl. Radio Sci. Meet. APSURSI 2018 — Proc*, Vol. 2, 843–844, 2018.
9. Zhang, L., Y. C. Jiao, Y. Ding, B. Chen, and Z. Bin Weng, "CPW-fed broadband circularly polarized planar monopole antenna with improved ground-plane structure," *IEEE Trans. Antennas Propag.*, Vol. 61, No. 9, 4824–4828, 2013.

10. Dong, Y. and T. Itoh, "Planar ultra-wideband antennas in Ku- and K-band for the pattern or polarization diversity applications," *IEEE Trans. Antennas Propag.*, Vol. 60, No. 6, 2886–2895, 2012.
11. Beaskoetxea, U., A. E. Torres-Garcia, and M. Beruete, "Ku-band low-profile asymmetric Bull's-eye antenna with reduced sidelobes and monopole feeding," *IEEE Antennas and Wireless Propagation Letters*, Vol. 17, No. 3, 401–404, 2018.
12. Yeoh, W. S. and W. S. T. Rowe, "A UWB conical monopole antenna for multiservice wireless applications," *IEEE Antennas and Wireless Propagation Letters*, Vol. 18, 1085–1088, 2015.
13. Pascale, V., D. Maiarelli, L. D'Agristina, and N. Gatti, "Design and qualification of Ku-band-radiating chains for receiving active array antennas of flexible telecommunication satellites," *Int. J. Microw. Wirel. Technol.*, Vol. 12, No. 6, 487–503, 2020.
14. Mei, L., L. Lang, N. Zhang, Y. Li, Y. Zhou, S. Chu, Y. Liu, and J. Yang, "A Ku-band conformal half-Yagi antenna for microwave communication," *2019 Photonics & Electromagnetics Research Symposium — Fall (PIERS — Fall)*, 1980–1986, Xiamen, China, 2019.
15. Oskouei, H. R. D., A. R. Dastkhosh, A. Mirtaheri, and M. Naseh, "A small cost-effective super ultra-wideband microstrip antenna with variable band-notch filtering and improved radiation pattern with 5g/IoT applications," *Progress In Electromagnetics Research M*, Vol. 83, 191–202, 2019.
16. Nurhayati, N., A. M. De Oliveira, J. F. Justo, E. Setijadi, B. E. Sukoco, and E. Endryansyah, "A compact monopole antenna for super wideband applications," *Microw. Opt. Technol. Lett.*, Vol. 62, No. 2, 964–974, 2020.
17. Nurhayati, G. H., T. Fukusako, and E. Setijadi, "Mutual coupling reduction for a UWB coplanar vivaldi array by a truncated and corrugated slot," *IEEE Antennas and Wireless Propagation Letters*, Vol. 17, No. 12, 2284–2288, 2018.
18. Wen, B. J., L. Peng, X. F. Li, K. S. Mo, X. Jiang, and S. M. Li, "A low-profile and wideband unidirectional antenna using bandwidth enhanced resonance-based reflector for fifth generation (5G) systems applications," *IEEE Access*, Vol. 07, 27352–27361, 2019.
19. Yang, D., S. Liu, and D. Geng, "A miniaturized ultra-wideband Vivaldi antenna with low cross-polarization," *IEEE Access*, Vol. 05, 23352–23357, 2017.
20. Zhou, Y., F. Zhu, S. Gao, Q. Luo, L.Wen, Q. Wang, X. Yang, Y. Geng, and Z. Cheng, "Tightly coupled array antennas for ultra-wideband wireless systems," *IEEE Access*, Vol. 06, 61851–61866, 2018.
21. Wen, B. J., L. Peng, X. F. Li, K. S. Mo, X. Jiang, and S. M. Li, "A low-profile and wideband unidirectional antenna using bandwidth enhanced resonance-based reflector for fifth generation (5G) systems applications," *IEEE Access*, Vol. 07, 27352–27361, 2019.
22. Manohar, M., R. S. Kshetrimayum, and A. K. Gogoi, "Super wideband antenna with single-band suppression," *Int. J. Microw. Wirel. Technol*, Vol. 9, No. 1, 143–150, 2017.
23. Chen, K. R., C. Y. D. Sim, and J. S. Row, "A compact monopole antenna for super wideband applications," *IEEE Antennas and Wireless Propagation Letters*, Vol. 10, 488–491, 2011.
24. Elhabchi, M., M. N. Srifi, and R. Touahni, "A novel CPW-fed semi-circular triangular antenna with modified ground plane for super ultra wide band (UWB) applications," *Int. Symp. Adv. Electr. Commun. Technol. ISAECT 2018 — Proc.*, 1–5, 2019.
25. Seyfollahi, A. and J. Bornemann, "Printed-circuit monopole antenna for super-wideband applications," *12th European Conference on Antennas and Propagation (EuCAP), 2018*, 1–5, 2018.
26. Manohar, M., R. S. Kshetrimayum, and A. K. Gogoi, "Printed monopole antenna with tapered feed line, feed region and patch for super wideband applications," *IET Microwaves, Antennas Propag.*, Vol. 8, No. 1, 39–45, 2014.
27. Haupt, R. L., "Antenna arrays," *A Computational Approach*, Wiley Online Library, 2010.